VOLUME 36 NUMBER 10

ACCOUNTS of CHEMICAL RESEARCH®

OCTOBER 2003

Close Encounters of the Transient Kind: Protein Interactions in the Photosynthetic Redox Chain Investigated by NMR Spectroscopy

PETER B. CROWLEY† AND MARCELLUS UBBINK*

Leiden Institute of Chemistry, Leiden University, Gorlaeus Laboratories, P.O. Box 9502, 2300 RA Leiden, The Netherlands

Received January 21, 2003

ABSTRACT

Plastocyanin and cytochrome c_6 function as electron shuttles between cytochrome *f* and photosystem I in the photosynthetic redox chain. To transfer electrons the partners form transient complexes, which are remarkably short-lived (milliseconds or less). Recent nuclear magnetic resonance studies have revealed details of the molecular interfaces found in such complexes. General features include a small binding site with a hydrophobic core and a polar periphery, including some charged residues. Furthermore, it was found that the interactions are relatively nonspecific. The structural information, in combination with kinetic and theoretical analyses of protein complexes, provides new insight into the nature of transient protein interactions.

Why Transient?

Biological energy transduction is performed by chains of redox proteins, which provide a path for the controlled flow of electrons. In these processes, such as photosynthesis and oxidative phosphorylation, soluble redox proteins facilitate electron transport between membrane-bound protein complexes. High-turnover conditions are necessary to sustain a continuous electron current, and therefore the interactions between the chain components occur transiently.[1,2] To maintain a transient interaction, the dissociation rate constant of the complex must be high ($k_{off} \geq 10^3$ s^{-1}). The association rate constants (k_{on}) are also high and have been experimentally determined to be in the range of 10^7-10^9 M^{-1}s^{-1} for electron-transfer partners.[3−6] Considering the high k_{on} and k_{off} values, this results in equilibrium association constants ($K_a = k_{on}/k_{off}$) in the μM$^{-1}-$mM^{-1} range. This raises the question of how sufficient affinity and specificity can be achieved to enable the formation of reactive electron-transfer complexes.

The fact that redox proteins are reactive toward multiple partners is an essential consideration in the subject of transient protein interactions.[7−9] Complex formation involves binding sites, which must be able to recognize and bind different molecular surfaces with comparable affinities. If the binding site was stereochemically optimized toward one partner, it would reduce the affinity for other partners.[7,8] This would result in tight binding with one partner and very weak binding to the other, effectively inhibiting turnover.

In this Account we address the issues of specificity and affinity in relation to the electron transfer proteins involved in the photosynthetic redox chain. The redox reactions between these partners have been investigated extensively using optical methods and mutagenesis. Recent nuclear magnetic resonance (NMR) studies provide structural detail of the complex interfaces and suggest some general features that are responsible for the high k_{off} and confer the ability to interact transiently.

* Corresponding author. E-mail: m.ubbink@chem.leidenuniv.nl.

† Present Address: Instituto de Tecnologia Química e Biológica, Universidade Nova de Lisboa, Av. Da República, Apartado 127, 2781 901 Oeiras, Portugal.

Peter Crowley was born in 1977 in Dublin, Ireland. He received his B.Sc. from University College Dublin in 1998 and in the same year began post-graduate work in the Metallo-Protein group of Gerard W. Canters at Leiden University. In November 2002 he earned his Ph.D., and he currently holds a Marie Curie Fellowship at ITQB, Lisbon.

Marcellus Ubbink was born in 1965 in Barneveld, The Netherlands. He graduated from Utrecht University in 1989 and earned his Ph.D. from Leiden University in 1994. After postdoctoral research at Cambridge University with Derek S. Bendall, he joined the faculty at the Leiden Institute of Chemistry in 1997. Currently, he is the holder of a VIDI Fellowship awarded by the Netherlands Organisation for Scientific Research. His research interests are in the area of transient protein interactions.

10.1021/ar0200955 CCC: $25.00
Published on Web 07/30/2003

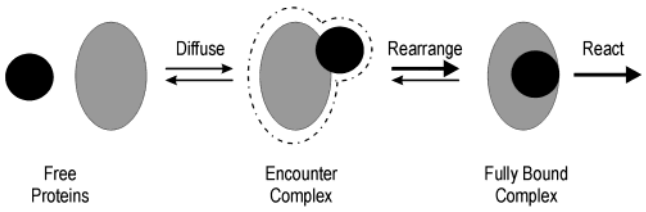

FIGURE 1. Schematic representation of transient complex formation, illustrating the three-step mechanism of Hervás et al.[4] Long-range, electrostatic interactions produce an ensemble of preoriented configurations. Subsequently, the partner proteins rearrange to the optimal configuration by surface diffusion. Once the specific complex is formed, electron transfer occurs and the products dissociate.

Plastocyanin and Cytochrome c_6

During photosynthesis, electron transport between the cytochrome *bf* complex and photosystem I (PSI) is maintained by either plastocyanin (Pc) or cytochrome c_6 (cytc_6). Depending on the relative availability of copper and iron, Pc (a β-sheet cupredoxin)[10] and cytc_6 (an α-helical heme-protein)[11] are alternately expressed in certain algae and cyanobacteria.[11,12] Although belonging to different protein classes, they perform equivalent reactions with common partners. Such a functional convergence demands that the reactive portions of Pc and cytc_6 are adequately adapted toward both partners. As expected, the two proteins have comparable redox potentials.[11] Furthermore, they are of similar size and have comparable surface characteristics, despite gross differences in primary, secondary, and tertiary structures.[13−15] The most explicit feature of this functional convergence is the parallel variation of the isoelectric point (p*I*) of both proteins in different organisms, being acidic in algae while ranging from acidic to basic in cyanobacteria.[11,14]

Reduction of PSI by Pc and cytc_6 has proved to be a model system for interprotein electron-transfer studies.[4,16−19] Similarly, reduction of Pc by cyt*f* has been extensively studied.[6,20−23] Kinetic and mutagenesis studies have highlighted the role of electrostatics in complex formation. The prominent acidic patches conserved in plant and algal variants of Pc have been identified as crucial for electrostatic docking to a positively charged site on both cyt*f* and PSI.[14,19,20] It is essential to note, however, that mutations affecting k_{on} are not restricted to the complex interface.[24] A charge mutation distorts the electrostatic potential of the protein as a whole, which in turn can influence the association with partner proteins. Mutations in the hydrophobic patches of Pc and cytc_6 have also revealed the importance of these surfaces for the interactions with cyt*f* and PSI.[16,23,26] On the basis of such studies, Hervás et al. have devised a three-step model for interprotein electron transfer[4] (Figure 1). Long-range, electrostatic interactions generate an ensemble of preoriented complexes. Subsequently, under the guide of hydrophobic interactions, the reactive configuration is obtained via surface diffusion. In some cases the rearrangement step can be detected by laser flash photolysis experiments.[4] This mechanism, which avoids the "lock-and-key" formalism,[27] is in line with the Velcro model proposed earlier.[8] According to McLendon, partner proteins possess a number of broadly complementary charged and hydrophobic patches, which can overlap in various orientations and contribute to a diffuse binding site.[8]

While the global features of the electron transfer reaction and the potential role of individual residues have been recognized through kinetic and mutagenesis studies, these methods provide little structural information. In this respect, NMR spectroscopy provides highly complementary tools for identification and characterization of the complex interface.

NMR Spectroscopy and Transient Protein Complexes

NMR spectroscopy is particularly suited to the study of low affinity complexes, which might not be amenable to cocrystallization. In the chemical-shift perturbation experiment, a ^{15}N-labeled protein is selectively monitored during a titration with the unlabeled partner.[28−30] Complex formation gives rise to changes in the chemical environment of nuclei at the interface, such that the chemical shift (δ) of these nuclei differs between the bound (δ_{bound}) and free (δ_{free}) forms. The effects on the NMR spectrum are dependent on the lifetime of the complex. In the slow exchange limit, the complex lifetime is long relative to the difference (in rad s^{-1}) between δ_{bound} and δ_{free} ($\Delta\delta_{Max}$), and the bound and free nuclei resonate at δ_{bound} and δ_{free}, respectively. In the fast exchange limit, the lifetime is shorter than $\Delta\delta_{Max}$, and a single resonance is observed at the weighted average of δ_{bound} and δ_{free}. During a titration, the ratio of the two proteins is altered and thus the fraction of bound protein changes. In the case of fast exchange, this results in a proportional shift of the average peak; as the fraction of bound protein increases, δ approaches δ_{bound}, and thus the change in δ ($\Delta\delta_{Bind}$) approaches $\Delta\delta_{Max}$. The lifetime is determined by k_{off}. Generally, in transient complexes of electron-transfer proteins, the fast exchange regime is observed, so $k_{off} > \Delta\delta_{Max}$ for most peaks (note that $\Delta\delta_{Max}$ is different for each nucleus), and a lower limit for k_{off} can be set at ∼200 s^{-1}.

When $\Delta\delta_{Bind}$ is plotted as a function of the molar ratio of the reactants, it is possible to derive binding curves for complex formation and hence the stoichiometry and affinity can be determined (Figure 2). Panel A illustrates $|\Delta\delta_{Bind}|$ for several amide nuclei of Pc when titrated with cyt*f*. With increasing [cyt*f*]:[Pc], the fraction of bound Pc increases and $\Delta\delta_{Bind}$ approaches $\Delta\delta_{Max}$. In panel B, $|\Delta\delta_{Bind}|$ is plotted for residues of cytc_6 upon titration into cyt*f*. With increasing [cytc_6]:[cyt*f*] the fraction of bound cytc_6 decreases, so the average peaks move toward δ_{free} and $\Delta\delta_{Bind}$ approaches zero. The percentage of bound protein can be calculated from the ratio of the experimentally observed $\Delta\delta_{Bind}$ and the fitted $\Delta\delta_{Max}$. To compare chemical-shift perturbation in different complexes, the shifts are extrapolated to the 100% bound form ($\Delta\delta_{Max}$), and the average chemical-shift perturbation ($\Delta\delta_{Avg}$) is calculated for each backbone amide using[28]

$$\Delta\delta_{Avg} = \sqrt{[(\Delta\delta N/5)^2 + \Delta\delta H^2]/2} \qquad (1)$$

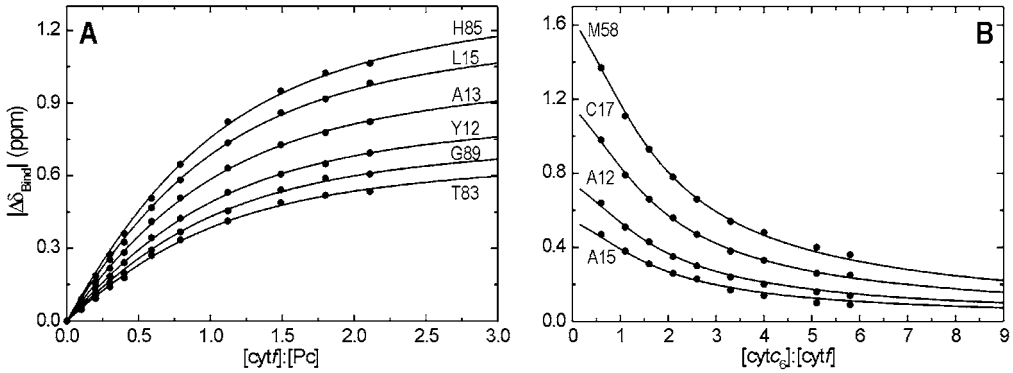

FIGURE 2. Binding curves for the interaction between *Phormidium* cyt*f* and (A) *Prochlorothrix* Pc[36] and (B) *Anabaena* cytc_6.[35] The data were fitted (nonlinear, least squares) to a one-site binding model,[20] with the protein ratio and $|\Delta\delta_{Bind}|$ as the independent and dependent variables, respectively. The binding constant (K_a) and the maximum chemical-shift change ($\Delta\delta_{Max}$) were the fitted parameters. A global fit was performed in which the curves were fitted simultaneously to a single K_a value, while the $\Delta\delta_{Max}$ for each resonance was allowed to vary. Binding constants of 6 ($\pm$2) $\times$ 10^3 M^{-1} and 8 ($\pm$2) $\times$ 10^3 M^{-1} were obtained for the complexes of *Phormidium* cyt*f* with *Prochlorothrix* Pc[36] and *Anabaena* cytc_6,[35] respectively.

Table 1. Transient Protein Interactions between Cyt*f* and Various Partner Proteins

partner proteins	p*I*	ratio	K_a (M^{-1})[a]	interface[b]	ref
cyt*f* (*Phormidium*)					
Phormidium Pc	4.8	1:1	$\sim 3 \times 10^2$	20H 8P 6C	34,36
Prochlorothrix Pc	8.0	1:1	6 ($\pm$2) $\times$ 10^3	24H 9P 7C	36
Anabaena cytc_6	9.0	1:1	8 ($\pm$2) $\times$ 10^3	25H 10P 5C	35
Synechococcus cytc_6	4.8	—[c]	—	—	35
Saccharomyces cyt*c*	9.7	2:1	$\sim 10^4/\sim 10^3$	12H 5P 5C	33
cyt*f* (*Brassica*)					
Spinacia Pc	3.8	1:1	$\sim 2 \times 10^4$	not determined	
			$\sim 7 \times 10^3$	18H 9P 8C	32

[a] Values of K_a were obtained from nonlinear, least-squares fits of binding curves derived from NMR titrations at pH 6.0, 10 mM ionic strength. Binding curves for the complex of plant cyt*f* and Pc were determined at 15 and 45 mM ionic strength (M. Ubbink, unpublised results, 1977). [b] The number and type of interface residues, for which a $\Delta\delta_{Bind}$ was observed, are quantified as (H)ydrophobic, (P)olar and (C)harged. [c] Complex formation was not detected.

where $\Delta\delta$N and $\Delta\delta$H are the changes in the ^{15}N and $^{1}H^{N}$ chemical shifts, respectively, when the protein is 100% bound. A complete picture of the interaction interface can be obtained by mapping $\Delta\delta_{Avg}$ to a surface representation of the protein, as will be illustrated in a later section.

In addition to chemical-shift perturbation, complex formation in the fast exchange regime is manifested as a general broadening of the resonances. The rotational correlation time of the complex is larger than that of the free proteins, resulting in an increase in the line widths of all resonances.[30] As with chemical shifts, in the fast exchange limit, the line width of the average resonance is the weighted average of the line widths of the free and bound forms.

Complex Formation between Cyt*f* and Partners, Pc, and Cytc_6

The results of NMR investigations with a soluble form of cyt*f*[31] from *Phormidium laminosum* are summarized in Table 1. The complex of cyt*f* and Pc from plants[32] is included for comparison. In all cases the free and bound forms were in fast exchange, indicative of the transient nature of these complexes.

Promiscuous Complex Formation. The most remarkable feature of Table 1 is the versatility of *Phormidium* cyt*f* (p*I* 4.8) interactions with both physiological and nonphysiological partners. Depending on the partner protein, binding constants ranging from $\sim 10^2$ to 10^4 M^{-1} were observed. Interestingly, the tightest complex was formed with the nonphysiological partner yeast cytochrome *c*.[33] This result highlights an essential difference between transient and static complexes. In static complexes the recognition and hence the binding affinity is optimized toward a specific partner. In transient complexes, the affinity is neglected in favor of high turnover, with the result that higher affinity complexes can be formed when a protein is "forced" to interact with nonphysiological partners. Such behavior does not conform to the lock and key formalism but is indicative of the degree of variability in the binding sites employed in transient complexes.

Only one of the five complexes with *Phormidium* cyt*f* (Table 1) is physiological, and yet three of the non-native partners have higher binding affinities. The origin of this increased binding affinity is probably from attractive electrostatic interactions, as suggested by the p*I* of the partner proteins. Increased electrostatic attraction will tend to promote k_{on}, and therefore K_a will be higher. Except in the extreme case of salt bridge formation, however, electrostatic interactions do not provide specificity in the fully bound complex and therefore cannot aid in the discrimination between native and "near-native" partners. It is important to bear in mind that the p*I* of a protein is not always a useful indicator of reactivity. A

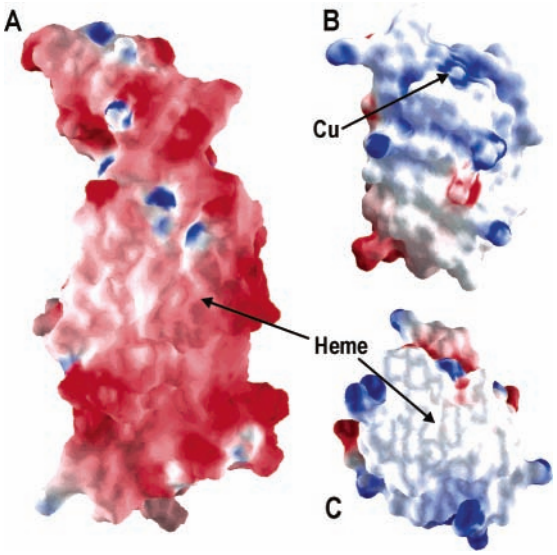

FIGURE 3. Electrostatic potential surfaces of (A) *Phormidium* cyt*f*,[58] (B) *Prochlorothrix* Pc[59], and (C) *Anabaena* cytc_6 (structural model[35] built in Swiss-Model[60]). The locations of the heme groups and the copper center are indicated with arrows. Pc and cytc_6 are oriented as in Figure 5. All images were created with a color ramp for positive (blue) or negative (red) surface potentials saturating at 10 kT. The potentials were calculated, for formal charges only, and surfaces were rendered in GRASP.[61]

comparison of *Phormidium* Pc and *Synechococcus elongatus* cytc_6, which have the same net charge and p*I*, demonstrates this point. Although the bulk charge properties are similar, their ability to form a complex with cyt*f* differs markedly. The absence of favorable electrostatics between *Phormidium* Pc and cyt*f* is reflected in the extremely low binding constant of this complex.[34] Yet a specific complex is formed, while *Synechococcus* cytc_6 has no detectable affinity for cyt*f*.[35]

Analogous Complexes with Diverse Partners. Another interesting result is the analogous reactivity of *Prochlorothrix* Pc and *Anabaena* cytc_6, which both form well-defined complexes with *Phormidium* cyt*f*.[35,36] The arrangement of basic residues in the vicinity of the redox centers is similar in both Pc and cytc_6 (Figure 3). This has important consequences for the interactions with the acidic cyt*f*. Binding curves for the interaction of cyt*f* and Pc are plotted in Figure 2A. Fitting the curves to a 1:1 binding model[20] yielded a binding constant of 6(2) $\times$ 10^3 M^{-1}.[36] A $\Delta\delta_{Avg} \geq 0.025$ ppm was obtained for forty backbone amides in Pc (Figure 4A). When these chemical-shift changes were mapped onto a surface representation of *Prochlorothrix* Pc, the binding site could be readily identified.[36] The affected residues are localized on one end of the molecule, resulting in a well-defined binding site, centered on the exposed copper ligand, His85 (Figure 5A). The immediate surroundings of the His85 side chain is composed of hydrophobic residues, while polar and charged groups are found toward the extremities of the binding site.

A binding constant of 8(2) $\times$ 10^3 M^{-1} was determined for the complex of *Anabaena* cytc_6 and cyt*f* (Figure 2B).[35] Coincidentally, the number of backbone amides for which a significant $\Delta\delta_{Avg}$ was observed was also 40 in this case (Figure 4B). The chemical-shift map identifies the interface as a contiguous patch surrounding the exposed methyls of the heme (Figure 5B). Again the binding site is composed mainly of hydrophobic side chains while polar and charged residues occur on the periphery.[35] The prevalence of electrostatic attraction in the complex was evidenced from the ionic strength dependence of $\Delta\delta_{Bind}$ (data not shown). As the salt concentration was increased, $\Delta\delta_{Bind}$ decreased, and at 0.2 M NaCl, the $\Delta\delta_{Bind}$ was zero for most resonances.[35] Similar ionic strength effects were observed in the complex with *Prochlorothrix* Pc.[36]

Despite their gross structural differences, it is evident that *Prochlorothrix* Pc and *Anabaena* cytc_6 experience a comparable binding affinity and utilize binding sites of similar composition for the interaction with cyt*f*.

Distinct Mechanisms of Interprotein Electron Transfer. From the kinetic and NMR studies, it can be concluded that different organisms utilize distinct mechanisms of inter-protein electron transfer. The interaction of plant Pc and cyt*f* is guided by complementary charged patches resulting in a rapid k_{on} at low ionic strength.[16,20,22,32]

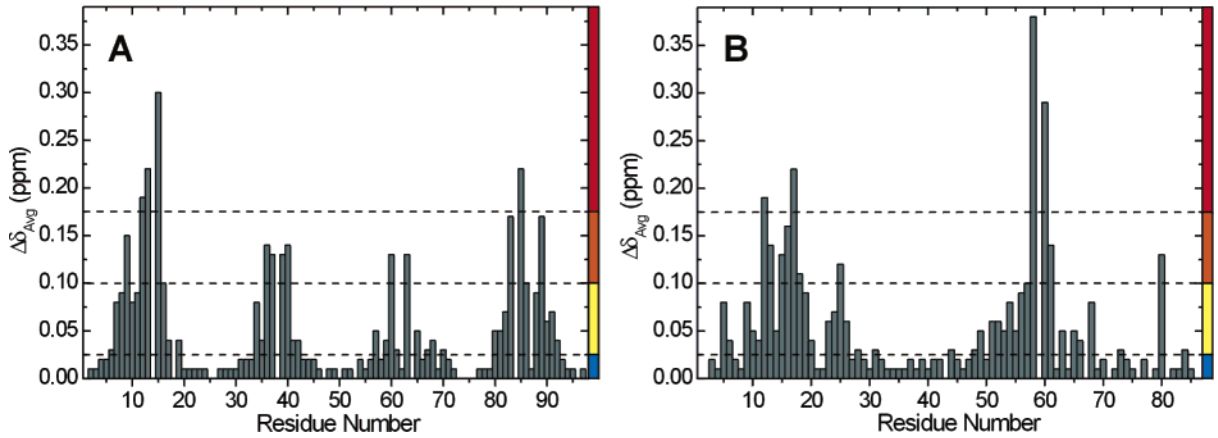

FIGURE 4. The average chemical-shift perturbation ($\Delta\delta_{Avg}$) extrapolated to the 100% bound form, experienced by *Prochlorothrix* Pc and *Anabaena* cytc_6 in complex with *Phormidium* cyt*f*. The color bars indicate the $\Delta\delta_{Avg}$ categories; insignificant $<$ 0.025 ppm, small $<$ 0.100 ppm, medium $<$ 0.175 ppm, and large $<$ 0.350 ppm, for chemical-shift mapping onto surface representations of the two proteins in Figure 5. Note the similarity in the magnitude of the shifts observed in both complexes.

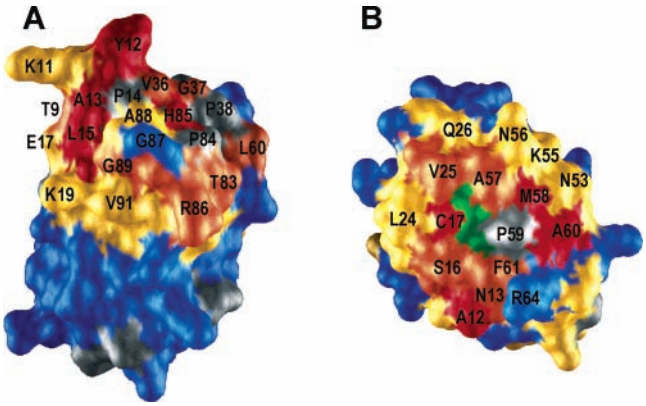

FIGURE 5. Chemical-shift perturbation mapping of (A) *Prochlorothrix* Pc[36] and (B) *Anabaena* cytc_6,[35] in the presence of *Phormidium* cyt*f*. Residues are colored according to the categories in Figure 4. Prolines are colored gray. The heme group of *Anabaena* cytc_6 is colored green.

At high ionic strength, k_{on} decreases strongly due to electrostatic screening.[20] In contrast, the Pc−cyt*f* complex from *Phormidium* relies primarily on hydrophobic interactions[6,34], and consequently the reaction rate constant is lower. However, since the cyanobacterial complex has a weak ionic strength dependence,[6,34] the reaction rate is much higher than the plant system at high ionic strength, and comparably fast under physiological conditions.[6]

Another example of distinct mechanisms is given by the interactions of cyt*f* and cytc_6. The results presented above indicate that cyt*f* forms a well-defined complex with *Anabaena* cytc_6.[35] *Synechococcus* cytc_6, however, does not form a complex (Table 1), though there is some evidence for a very weak interaction.[35,37] Similar results have been observed for the reactivity of *Anabaena* and *Synechococcus* cytc_6 toward their respective PSI partners, suggesting that *Anabaena* cytc_6 reacts via formation of well-defined complexes,[4] while *Synechococcus* cytc_6 employs a collision mechanism.[38]

Contributing Factors to Transient Interactions

As mentioned in the Introduction, transient complexes are characterized by both high k_{on} and k_{off} rates. In an attempt to understand the promiscuity of transient protein interactions, it is necessary to discuss the factors that influence (transient) complex formation.[39]

The Encounter Complex. The solvent cage effect, as postulated by Adam and Delbrück,[40] provides the first clues to understanding the fast k_{on}. Upon collision, two proteins occupy the same solvent shell even in the absence of intermolecular attraction. Trapped by the surrounding water molecules, the proteins rapidly collide with one another.[41] This nonspecific association, involving several collisions, is called the encounter complex.[41] Northrup and Erickson have confirmed, using Brownian dynamics (BD), that there is a high probability of recolliding after the initial collision.[42] Moreover, the lifetime of the encounter was shown to be on the order of the rotational correlation time of the proteins. This enables the proteins to sample different conformations within the encounter complex.[42]

Electrostatics. Long-range electrostatic interactions complement the solvent cage effect in several ways.[43,44] While Coulombic attraction between oppositely charged reactants accelerates the rate of bimolecular association, it can also produce a preorientation of the diffusing reactants as suggested by Matthew et al.[45] In some cases co-evolution has resulted in complementary charged patches that steer the proteins into reactive collisions. This effect is particularly pronounced in barnase−barstar[46] and Pc−cyt*f*[20] interactions. Although representative of static and transient complexes, respectively, these have similar association rate constants ($>10^8$ $M^{-1}s^{-1}$) which decrease dramatically as the ionic strength is increased.[20,46] Using BD simulations Wade and co-workers have obtained good agreement between calculated and experimental association rates for these interacting pairs. Furthermore, the ionic strength dependence and the effect of charge mutations on the association rate were successfully modeled.[47,48]

Along with assisting bimolecular association, electrostatics can also prolong the lifetime of the encounter complex through nonspecific attraction.[43,44] The potential contribution of electrostatics to the affinity of the complex appears, however, to be offset by desolvation.[44,49] Elcock et al. have demonstrated that BD calculated rates are similar to experimental association rates only when a penalty term for desolvation of charged groups at the interface is included in the calculation.[49] While electrostatic attractions promote the kinetics of binding, the contribution to the thermodynamics of binding does not seem to be strongly favorable.[44,49]

Hydrophobics. Whereas electrostatic interactions often contain information for the initial recognition event, formation of the fully bound complex is determined by other interactions. Upon association, attendant water molecules, which form a layer around the protein surface, are liberated.[50] The increased entropy of the released water molecules compensates for the loss of rotational and translational entropy of the proteins and provides a driving force for complex formation. Again, BD calculations provide insight into the role of desolvation.[51,52] The initial encounter is accompanied by partial desolvation of the protein surfaces. When the partners rearrange to the fully bound complex, interfacial contacts are increased, and a greater volume of water is expelled. Although desolvation is a short-range effect, Camacho et al. have demonstrated that it can lead to substantial increases in k_{on} when complementary electrostatics are absent or weak.[52] Rate enhancement occurs on the basis that desolvation favors entrapment and guides the proteins into reactive configurations. This effect is likely to be particularly pronounced for redox proteins, which have well-defined hydrophobic patches surrounding their redox centers.[7,53]

The Size of the Complex Interface. Structural analysis of Pc−cyt*f* complexes indicates that a surface area of approximately 600 Å^2 is buried per partner in the complex

interface.[32,34] Comparison of the chemical-shift maps (Figure 5) suggests that a similar surface area is buried in the cytc_6−cyt*f* complex. According to the classification of Lo Conte et al. complexes that bury ~600 Å^2 per partner are considered "small-size" interfaces.[54] Although poorly represented in the Protein Databank, it has been suggested that the small-size interface is a contributing factor to the transient nature of such complexes.[39,54]

Using the Smoluchowski equation,[55] the diffusion-controlled association rate is calculated to be $>10^9$ M^{-1}s^{-1} in the size range of proteins.[41,42,51] Active sites in proteins are confined to a specific region of the structure, the steric accessibility of which represents a minute fraction of the molecular surface. Therefore, in the limit of stochastic motion, the probability of productive encounters is expected to be a 1000-fold lower.[24,41,42] The predicted rate is based on the assumption that productive binding involves <1% of the protein surface. In agreement with this assumption, Pc requires electronic coupling through the exposed histidine ligand of the copper, which accounts for 0.4% of the molecular surface. The surface involved in the complex interface (~600 Å^2), however, represents 12% of the surface area of Pc and consists of a conserved hydrophobic patch.[34] Furthermore, the histidine ligand protrudes through the center of the patch. This nonpolar binding site, which provides hydrophobic free energy in favor of association, guides the protein toward the reactive conformation.[52] Thus, collisions resulting in partial overlap can lead to a productive complex, as suggested by Camacho *et al.*[52] and will increase k_{on} relative to the predicted ~10^6 M^{-1}s^{-1}. This effect has been observed experimentally in the case of the nonelectrostatic Pc-cyt*f* complex from *Phormidium* ($k_{on} > 10^7$ M^{-1} s^{-1}).[6]

The Character of the Complex Interface. In 1894 Fischer wrote: "enzyme and glucoside must fit one another like a lock and key in order to exert a chemical effect on each other".[27] Whereas the interfaces in static complexes can be considered an extension of this principle, the evidence accumulated in this Account and elsewhere indicates that transient complex formation is not highly specific.[7−9,36] In particular, the structurally diverse Pc and cytc_6 can form complexes of identical affinity with cyt*f*.[35,36] Although discrete binding sites have been identified (Table 1), the formation of stereochemically optimized interfaces appears unnecessary.[9,36] This concept is supported by the fact that transient complex formation occurs readily between nonphysiological partners.[33]

Of the five complexes for which a binding map could be determined (Table 1), the interface consists on average of 57% hydrophobic, 24% polar, and 19% charged residues. While this result agrees qualitatively with the composition of the accessible surface area of small globular proteins,[56] there is an important distinction to be made. The character of the interface is manifestly heterogeneous, consisting of a core of hydrophobic side chains in the immediate vicinity of the redox center, while polar and charged side chains occur on the periphery (Figure 5). Desolvation of the interface is likely to be less favorable in the presence of polar and charged residues. Therefore, the hydrophobic free energy gain upon association will be reduced and this contributes to the transient nature of such complexes. If the side chains are not close packed,[9,36,54] the interface will be poorly sealed and remains permeable to water molecules which can "rewet" the binding site and disrupt the complex. Furthermore, van der Waals contacts across the interface cannot be maximized and therefore their contribution to the binding affinity will not be optimal. Together, these features promote fast dissociation and enable the transient interaction.

Conclusion and Outlook

It can be concluded that, in general, electron-transfer proteins interact via small binding patches, which consist of a hydrophobic center and a polar/charged periphery. The small size of the interface and the absence of close packing lowers both the specificity and the affinity, thus contributing to the high k_{off}. Desolvation of the hydrophobic patch favors entrapment and drives productive complex formation (k_{on}). While charged residues can enhance k_{on} through long-range electrostatic steering, they do not contribute much to short-range specificity. When electrostatic attraction is weak or absent, the resulting binding constant is extremely low. The balance between the hydrophobic effect and electrostatic interactions (both attractive and repulsive) helps to explain why in some organisms the reaction proceeds via complex formation, while in others the same reaction is collisional.[35] In the latter case, it is likely that the electrostatic interaction is predominantly repulsive thus prohibiting complex formation.

NMR spectroscopy provides essential structural information concerning transient protein complexes. The results are highly complementary to and aid the explanation of kinetic and mutagenesis studies. Even more valuable information can be obtained when not only the complex interface, but also the relative orientation of the proteins is determined. Developments with paramagnetic methods in our laboratory indicate that it is possible to obtain this information from long-range interprotein restraints, despite the low affinity of these complexes. Transient protein interactions are increasingly becoming the focus of research in many areas of biochemistry.[57] Continued structural characterization is vital therefore to understanding the subtlety and range of function in these complexes.

References

(1) Bendall, D. S. Interprotein electron transfer. In *Protein Electron Transfer*; Bendall, D. S., Ed.; Bios Scientific: Oxford, 1996; pp 43−64.
(2) Mathews, F. S.; Mauk, A. G.; Moore, G. R. Protein−protein complexes formed by electron-transfer proteins. In *Protein−Protein Recognition*; Kleanthous, C., Ed.; Oxford University Press: New York, 2000; pp 60−101.
(3) Kang, C. H.; Ferguson-Miller, S.; Osheroff, N.; Margoliash, E. Steady-state kinetics and binding of eukaryotic cytochromes *c* with yeast cytochrome *c* peroxidase. *J. Biol. Chem.* **1977**, *252*, 919−926.

(4) Hervás, M.; Navarro, J. A.; Díaz, A.; Bottin, H.; De la Rosa, M. A. Laser-flash kinetic-analysis of the fast-electron transfer from plastocyanin and cytochrome c_6 to photosystem I − experimental evidence on the evolution of the reaction mechanism. *Biochemistry* **1995**, *34*, 11321−11326.

(5) Sétif, P. Q. Y.; Bottin, H. Laser-flash absorption-spectroscopy study of ferredoxin reduction by photosystem I − spectral and kinetic evidence for the existence of several photosystem I−ferredoxin complexes. *Biochemistry* **1995**, *34*, 9059−9070.

(6) Schlarb-Ridley, B. G.; Bendall, D. S.; Howe, C. J. Role of electrostatics in the interaction between cytochrome *f* and plastocyanin of the cyanobacterium *Phormidium laminosum*. *Biochemistry* **2002**, *41*, 3279−3285.

(7) Williams, P. A.; Fulop, V.; Leung, Y. C.; Chan, C.; Moir, J. W. B.; Howlett, G.; Ferguson, S. J.; Radford, S. E.; Hajdu, J. Pseudospecific docking surfaces on electron-transfer proteins as illustrated by pseudoazurin, cytochrome c_{550} and cytochrome cd_1 nitrate reductase. *Nat. Struct. Biol.* **1995**, *2*, 975−982.

(8) McLendon, G. Control of biological electron-transfer via molecular recognition and binding − the Velcro model. *Struct. Bond.* **1991**, *75*, 159−174.

(9) Jeng, M.-F.; Englander, S. W.; Pardue, K.; Rogalskyj, J. S.; McLendon, G. Structural dynamics in an electron-transfer complex. *Nat. Struct. Biol.***1994**, *1*, 234−238.

(10) Sigfridsson, K. Plastocyanin, an electron-transfer protein. *Photosynth. Res.* **1998**, *57*, 1−28.

(11) Kerfeld, C.A.; Krogmann, D. W. Photosynthetic cytochromes c in cyanobacteria, algae, and plants. *Annu. Rev. Plant Physiol.* **1998**, *49*, 397−425.

(12) Wood, P. M. Interchangeable copper and iron proteins in algal photosynthesis. Studies on plastocyanin and cytochrome *c*-552 in *Chlamydomonas*. *Eur. J. Biochem.* **1978**, *87*, 9−19.

(13) Frazão, C.; Soares, C. M.; Carrondo, M. A.; Pohl, E.; Dauter, Z.; Wilson, K. S.; Hervás, M.; Navarro, J. A.; De la Rosa, M. A.; Sheldrick, G. M. *Ab initio* determination of the crystal-structure of cytochrome c_6 and comparison with plastocyanin. *Structure* **1995**, *3*, 1159−1169.

(14) Navarro, J. A.; Hervás, M.; De la Rosa, M. A. Co-evolution of cytochrome c_6 and plastocyanin, mobile proteins transferring electrons from cytochrome b_6f to photosystem I. *J. Biol. Inorg. Chem.* **1997**, *2*, 11−22.

(15) Ullmann, G. M.; Hauswald, M.; Jensen, A.; Kostíc, N. M.; Knapp, E. W. Comparison of the physiologically equivalent proteins cytochrome c_6 and plastocyanin on the basis of their electrostatic potentials. *Biochemistry* **1997**, *36*, 16187−16196.

(16) Nordling, M.; Sigfridsson, K.; Young, S.; Lundberg, L. G.; Hansson, Ö. Flash-photolysis studies of the electron-transfer from genetically modified spinach plastocyanin to photosystem I. *Febs Lett.* **1991**, *291*, 327−330.

(17) Medina, M.; Diaz, A.; Hervás, M.; Navarro, J. A.; Gomez-Moreno, C.; De la Rosa M. A.; Tollin, G. A comparative laser-flash absorption-spectroscopy study of *Anabaena* PCC-7119 plastocyanin and cytochrome c_6 by photosystem I particles. *Eur. J. Biochemistry* **1993**, *32*, 1133−1138.

(18) Haehnel, W.; Jansen, T, Gause, K.; Klosgen, R. B.; Stahl, B.; Michl, D.; Huvermann, B.; Karas, M.; Herrmann, R. G. Electron-transfer from plastocyanin to photosystem I. *EMBO J.* **1994**, *13*, 1028−1038.

(19) Hippler, M.; Drepper, F.; Haehnel, W.; Rochaix, J. D. The N-terminal domain of PsaF: Precise recognition site for binding and fast electron transfer from cytochrome c_6 and plastocyanin to photosystem I of *Chlamydomonas reinhardtii*. *Proc. Natl. Acad. Sci. U.S.A.* **1998**, *95*, 7339−7344.

(20) Kannt, A.; Young, S.; Bendall, D. S. The role of acidic residues of plastocyanin in its interaction with cytochrome *f*. *BBA-Bioenergetics* **1996**, *1277*, 115−126.

(21) Meyer, T. E.; Zhao, Z. G.; Cusanovich, M. A.; Tollin, G. Transient kinetics of electron-transfer from a variety of *c*-type cytochromes to plastocyanin. *Biochemistry* **1993**, *32*, 4552−4559.

(22) Soriano, G. M.; Ponamarev, M. V.; Piskorowski, R. A.; Cramer, W. A. Identification of the basic residues of cytochrome *f* responsible for electrostatic docking interactions with plastocyanin in vitro: Relevance to the electron-transfer reaction in vivo. *Biochemistry* **1998**, *37*, 15120−15128.

(23) Illerhaus, J.; Altschmied, L.; Reichert, J.; Zak, E.; Herrmann, R. G.; Haehnel, W. Dynamic interaction of plastocyanin with the cytochrome *bf* complex. *J. Biol. Chem.* **2000**, *275*, 17590−17595.

(24) Schreiber, G.; Fersht, A. R.Rapid, electrostatically assisted association of proteins. *Nat. Struct. Biol.* **1996**, *3*, 427−431.

(25) Hervás, M.; Navarro, J. A.; Díaz, A.; De la Rosa, M. A. Comparative thermodynamic analysis by laser-flash absorption spectroscopy of photosystem I reduction by plastocyanin and cytochrome c_6 in *Anabaena* PCC 7119, *Synechocystis* PCC 6803, and spinach. *Biochemistry* **1996**, *35*, 2693−2698.

(26) Molina-Heredia, F. P.; Díaz-Quintana, A.; Hervás, M.; Navarro, J. A.; De la Rosa, M. A. Site-directed mutagenesis of cytochrome c_6 from *Anabaena* species PCC 7119 − Identification of surface residues of the hemeprotein involved in photosystem I reduction. *J. Biol. Chem.* **1999**, *274*, 33565−33570.

(27) Fischer, E. Einfluss der Configuration aus der Wirkung der Enzyme. *Ber. Dtsch. Chem. Ges.* **1894**, *27*, 2985−2993.

(28) Grzesiek, S.; Bax, A.; Clore, G. M.; Gronenborn, A. M.; Hu, J.-S.; Kaufman, J.; Palmer, I.; Stahl, S. J.; Wingfield, P. T. The solution structure of HIV-1 Nef reveals an unexpected fold and permits delineation of the binding surface for the SH3 domain of Hck tyrosine protein kinase. *Nat. Struct. Biol.* **1996**, *3*, 340−345.

(29) Arnesano, F.; Banci, L.; Bertini, I.; Cantini, F.; Ciofi-Baffoni, S.; Huffman, D. L.; O′ Halloran, T. V. Characterization of the binding interface between the copper chaperone Atx1 and the first cytosolic domain of Ccc2 ATPase. *J. Biol. Chem.* **2001**, *276*, 41365−41376.

(30) Zuiderweg, E. R. P. Mapping protein−protein interactions in solution by NMR Spectroscopy. *Biochemistry* **2002**, *41*, 1−7.

(31) Gray, J. C. Cytochrome *f* − structure, function and biosynthesis. *Photosynth. Res.* **1992**, *34*, 359−374.

(32) Ubbink, M.; Ejdeback, M.; Karlsson, B. G.; Bendall, D. S. The structure of the complex of plastocyanin and cytochrome *f*, determined by paramagnetic NMR and restrained rigid-body molecular dynamics *Structure* **1998**, *6*, 323−335.

(33) Crowley, P. B.; Rabe, K. S.; Worrall, J. A. R.; Canters, G. W.; Ubbink, M. The ternary complex of cytochrome *f* and cytochrome *c*: Identification of a second binding site and competition for plastocyanin binding. *ChemBioChem* **2002**, *3*, 526−533.

(34) Crowley, P. B.; Otting, G.; Schlarb-Ridley, B. G.; Canters, G. W.; Ubbink, M. Hydrophobic interactions in a cyanobacterial plastocyanin-cytochrome *f* complex. *J. Am. Chem. Soc.* **2001**, *123*, 10444−10453.

(35) Crowley, P. B.; Díaz-Quintana, A.; Molina-Heredia, F. P.; Nieto, P.; Sutter, M.; Haehnel, W.; De la Rosa, M. A.; Ubbink M. The interactions of cyanobacterial cytochrome c_6 and cytochrome *f* − characterized by NMR. *J. Biol. Chem.* **2002**, *277*, 48685−48689.

(36) Crowley, P. B.; Vintonenko, N.; Bullerjahn, G. S.; UbbinkM. Plastocyanin-cytochrome *f* interactions: The influence of hydrophobic patch mutations studied by NMR. *Biochemistry* **2002**, *41*, 15698−15705.

(37) Worrall, J. A. R.; Liu, Y.; Crowley, P. B.; Nocek, J. M.; Hoffman, B. M.; Ubbink, M. Myoglobin and Cytochrome b_5: A nuclear magnetic resonance study of a highly dynamic protein complex. *Biochemistry* **2002**, *41*, 11721−11730.

(38) Sutter, M.; Sticht, H.; Schmid, R.; Hörth, P.; Rösch, P.; Haehnel, W. Cytochrome c_6 from the thermophilic *Synechococcus elongatus*. In *Photosynthesis: From Light to Biosphere*; Mathis, P., Ed.; Kluwer Academic Publishers: Dordrecht, The Netherlands, 1995; pp 563−566.

(39) Wodak, S. J.; Janin, J. Structural basis of macromolecular recognition. *Adv. Protein Chem.* **2003**, *61*, 9−73.

(40) Adam, G.; Delbrück, M. Reduction of dimensionality in biological diffusion processes. In *Structural Chemistry and Molecular Biology*; Rich, A., Davidson, N., Eds.; Freeman: San Francisco, 1968; 198−215.

(41) Berg, O. G.; von Hippel P. H. Diffusion-controlled macromolecular interactions. *Annu. Rev. Biophys. Biophys. Chem.* **1985**, *14*, 131−160.

(42) Northrup, S. H.; Erickson, H. P. Kinetics of protein−protein association explained by Brownian dynamics computer simulation. *Proc. Natl. Acad. Sci. U.S.A.* **1992**, *89*, 3338−3342.

(43) Janin, J. The kinetics of protein−protein recognition. *Proteins* **1997**, *28*, 153−161.

(44) Sheinerman, F. B.; Norel, R.; Honig, B. Electrostatic aspects of protein−protein interactions. *Curr. Opin. Struct. Biol.* **2000**, *10*, 153−159.

(45) Matthew, J. B.; Weber, P. C.; Salemme, F. R.; Richards, F. M. Electrostatic orientation during electron transfer between flavodoxin and cytochrome *c*. *Nature* **1983**, *301*, 169−171.

(46) Schreiber, G.; Fersht, A. R. Interaction of barnase with its polypeptide inhibitor studied by protein engineering. *Biochemistry* **1993**, *32*, 5145−5150.

(47) Gabdoulline, R. R.; Wade, R. C. Simulation of the diffusional association of barnase and barstar. *Biophys. J.* **1997**, *72*, 1917−1929.

(48) De Rienzo, F.; Gabdoulline, R. R.; Menziani, M. C.; De Benedetti, P. G.; Wade, R. C. Electrostatic analysis and Brownian dynamics simulation of the association of plastocyanin and cytochrome *f*. *Biophys. J.* **2001**, *81*, 3090−3104.

(49) Elcock, A. H.; Gabdoulline, R. R.; Wade, R. C.; McCammon, J. A. Computer simulation of protein−protein association kinetics: acetylcholinesterase-fasciculin. *J. Mol. Biol.* **1999**, *291*, 149−162.

(50) Chothia, C.; Janin, J. Principles of protein−protein recognition. *Nature* **1975**, *256*, 705−708.
(51) Camacho, C. J.; Weng, Z. P.; Vajda, S.; DeLisi, C. Free energy landscapes of encounter complexes in protein−protein association. *Biophys. J.* **1999**, *76*, 1166−1178.
(52) Camacho, C. J.; Kimura, S. R.; DeLisi, C.; Vajda, S. Kinetics of desolvation-mediated protein−protein binding. *Biophys. J.* **2000**, *78*, 1094−1105.
(53) Adman, E. T. Copper protein structures. *Adv. Protein Chem.* **1991**, *42*, 145−197.
(54) Lo Conte, L.; Chothia, C.; Janin, J. The atomic structure of protein−protein recognition sites. *J. Mol. Biol.* **1999**, *285*, 2177−2198.
(55) Smoluchowski, M. V. Versuch einer mathematischen Theorie der Koagulationskinetik kolloider Loeschungen. *Z. Phys. Chem.* **1917**, *92*, 129−168.
(56) Miller, S.; Janin, J.; Lesk, A. M.; Chothia, C. Interior and surface of monomeric proteins. *J. Mol. Biol.* **1987**, *196*, 641−656.
(57) Nooren, I. M. A.; Thornton, J. M. Structural characterisation and functional significance of transient protein−protein interactions. *J. Mol. Biol.* **2003**, *325*, 991−1018.
(58) Carrell, C. J.; Schlarb, B. G.; Bendall, D. S.; Howe, C. J.; Cramer, W. A.; Smith, J. L. Structure of the soluble domain of cytochrome *f* from the cyanobacterium *Phormidium laminosum*. *Biochemistry* **1999**, *38*, 9590−9599.
(59) Babu, C. R.; Volkman, B. F.; Bullerjahn, G. S. NMR solution structure of plastocyanin from the photosynthetic prokaryote, *Prochlorothrix hollandica*. *Biochemistry* **1999**, *38*, 4988−4995.
(60) Guex, N.; Peitsch, M. C. Swiss-Model and the Swiss-Pdb Viewer: An environment for comparative protein modeling. *Electrophoresis* **1997**, *18*, 2714−2723.
(61) Nicholls, A.; Sharp, K.; Honig, B. Protein folding and association − insights from the interfacial and thermodynamic properties of hydrocarbons. *Proteins* **1991**, *11*, 281−296.

AR0200955